[11] Aldehyde **5** was prepared by diastereoselective alkylation of the Myers chiral amide **I** with iodide **II** [Eq. (2)]. A. G. Myers, L. McKinstry, *J. Org. Chem.* **1996**, *61*, 2428.

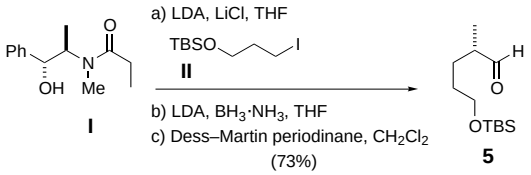

(2)

[12] The corresponding aldol addition with achiral aldehydes led to comparably high levels of 1,5-*anti* stereoinduction which indicates that chiral aldehyde **5** contributed only negligibly to 1,2-induction.
[13] D. A. Evans, K. T. Chapman, E. M. Carreira, *J. Am. Chem. Soc.* **1988**, *110*, 3560.
[14] A. De Mico, R. Margarita, L. Parlanti, A. Vescovi, G. Piancatelli, *J. Org. Chem.* **1997**, *62*, 6974.
[15] V. H. Dahanukar, S. D. Rychnovsky, *J. Org. Chem.* **1996**, *61*, 8317.
[16] Enol silane **6** was prepared from isovaleraldehyde [Eq. (3)].

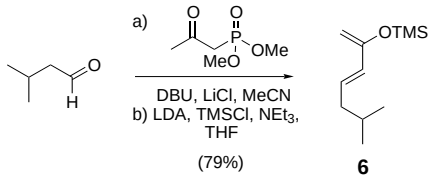

(3)

[17] I. Paterson, *Tetrahedron Lett.* **1979**, 1519.
[18] D. A. Evans, M. J. Dart, J. L. Duffy, M. G. Yang, *J. Am. Chem. Soc.* **1996**, *118*, 4322.
[19] O. Mitsunobu, *Synthesis* **1981**, 1. A Mitsunobu macrolactonization strategy was independently reported by Wipf et al.[4b] while this manuscript was in preparation.
[20] C. W. Jefford, J.-C. Rossier, J. Boukouvalas, P. Huang, *Helv. Chim. Acta* **1994**, *77*, 661.
[21] L. Banfi, G. Guanti, A. Basso, *Eur. J. Org. Chem.* **2000**, 939.
[22] N. F. Langille, L. A. Dakin, J. S. Panek, *Org. Lett.* **2002**, *4*, 2485.
[23] $[\alpha]_D^{20} = +40.0$ ($c = 0.29$, EtOH) [ref. [1], $[\alpha]_D^{20} = +41.0$ ($c = 0.29$, EtOH)]. For copies of ^1H and ^{13}C NMR spectra, see the Supporting Information.

Yttria-Zirconia Thin Films

Controlled Formation of Highly Ordered Cubic and Hexagonal Mesoporous Nanocrystalline Yttria–Zirconia and Ceria–Zirconia Thin Films Exhibiting High Thermal Stability**

*Eduardo L. Crepaldi, Galo J. de A. A. Soler-Illia, Anne Bouchara, David Grosso, Dominique Durand, and Clément Sanchez**

Zirconia-based mixed oxides are current targets of intensive research as a result of their applications in strategic technologies, such as yttria-stabilized zirconia (YSZ) in solid-oxide fuel cells (SOFCs),[1] and ceria–zirconia in the latest generation of automotive exhaust three-way catalysts,[2,3] the latter having the potential to be applied in the next generation of compact SOFCs.[3] In view of these applications, controlling the porosity of these systems is highly desirable. The "supramolecular template approach" offers precise control of the material porosity on the mesoscale (20–200 Å).[4] Ozin and co-workers[5] were the first to extend this method to the synthesis of YSZ by using cetyltrimethylammonium bromide (CTAB) templated glycolate-modified inorganic precursors. Gedanken and co-workers[6] reported the synthesis of mesoporous YSZ using metallic salts or oxides as inorganic sources and anionic surfactants as templates. All of these precipitation methods yield disordered wormlike mesoporous powders. However, to the best of our knowledge, periodically organized mesoporous ceria–zirconia and even yttria–zirconia materials are yet to be reported.

The present work reports the first examples of periodically organized mesoporous yttria–zirconia (YZ) and ceria–zirconia (CZ) ($R = M/(M+Z) = 0.05$–0.30, where Z is the amount of Zr and M is the amount of Y or Ce present in the material). Moreover, these materials are processed as thin films. The procedure is simple and reproducibly gives highly ordered mesoporous nonsilicate mixed oxides, which retain their structure (order and porosity) after crystallization of the inorganic walls and subsequent thermal treatment to temperatures as high as 700 °C. This advantageous one-step method can replace the usual precipitation of particles/deposition/

[*] Dr. C. Sanchez, Dr. E. L. Crepaldi, Dr. G. J. de A. A. Soler-Illia, A. Bouchara, Dr. D. Grosso
Laboratoire de Chimie de la Matière Condensée
UMR 7574, Université Pierre et Marie Curie (Paris VI)
4 place Jussieu, 75252 Paris CEDEX 05 (France)
Fax: (+33) 1-4427-4769
E-mail: clems@ccr.jussieu.fr
Dr. D. Durand
LURE Bât 209D, Centre Universitaire
B.P. 34, 91898 Orsay Cedex (France)

[**] This work was financially supported by the French Ministry of Research, CNRS, CNPq (Brazil, grant no. 200636/00-0), CONICET, and Fundación Antorchas (Argentina). Rhodia is greatly acknowledged for financial support of A.B.

Supporting information for this article is available on the WWW under http://www.angewandte.org or from the author.

sintering process that is applied to construct zirconia-based mixed-oxide porous coatings. The mesostructured hybrids (precursors to the mesoporous solids) were templated by poly(ethylene oxide) (EO) based amphiphilic block copolymers (ABCs), and were produced by an evaporation-induced self-assembly (EISA) derived method,[7] which uses anhydrous metal chlorides in ethanol/water solutions (see Experimental Section).

Figure 1 shows a schematic view of the film processing technique. Time-resolved small-angle X-ray scattering (SAXS) and interferometry analysis (SAXS beamline of Elettra, Trieste, Italy; details elsewhere[8]) showed that organization starts just after the drying line. A diffraction ring, characteristic of polyoriented domains, is initially observed. For SiO_2[9] and TiO_2-based[10] ABC-templated systems, the organization occurs through a "disorder-to-order" transition, which for the ZrO_2-based systems does not run to completion as a result of the formation of extended metal–oxo polymers, which "freeze" the intermediate worm-like mesophase. The quenched system has poor optical quality (see Figure 1a) after the first drying process (FD) at low relative humidity (RH). These freshly formed olated metal–oxo polymers (olation is kinetically favored[11]) can be "rearranged" by a short (10–20 s) water-vapor treatment (WVT), which promotes the diffusion of water within the coating to allow the reorganization of the organic species into a highly ordered mesophase. The second drying process (SD) then takes place homogeneously, which results in smooth crack-free coatings (see Figure 1b). This formation path takes place for all zirconia-based systems, and was also observed for Brij 58-templated mesostructured ZrO_2 films.[12]

At this stage, the inorganic framework is far from being fully condensed (see Supporting Information). We observed that one can take advantage of structural "flexibility" to tailor the final mesophase at a fixed template/inorganic molar ratio. Figure 2 shows 2D synchrotron SAXS patterns (recorded at the D43 line of LURE, Orsay, France; transmission mode, incidence of 4° to the substrate) that correspond to two different mesostructures obtained for different RHs during SD and aging. For pure ZrO_2, a 2D hexagonal mesostructure is obtained under all conditions. The loading of less acidic trivalent metal cations ($R = 5$–$30\,\%$) induces a higher flexibility of the inorganic framework and allows for the formation of cubic mesophases. The low tendency of such cations to condense in acidic media is likely to reduce the condensation rate and the extension of the ZrO_2-based inorganic polymers (creation of "dead ends"). In addition, the different size and coordination of these cations (when compared to the Zr^{4+} ion) can alter the polyhedral linking. Each of these effects can contribute, either individually or in association, to give a better adjustment of the inorganic framework to the more curved organic–inorganic interface of the cubic mesophase.[8b]

For films with R greater than 5% that were dried and aged under "dry" conditions (RH = 10%), the SAXS patterns show six defined spots that can be indexed as the {10} reflections of a 2D hexagonal (*P6m* space group) mesostructure (Figure 2a) with the channels, and more precisely the (01) planes, preferentially aligned parallel to the substrate. The same orientation has already been observed for CTAB or F127-templated 2D hexagonal mesoporous silica films.[9,13] The unit-cell parameters are displayed in Table 1. Drying and aging under a humid atmosphere (RH = 50%) favors the formation of a cubic mesophase (Figure 2b). The resulting SAXS patterns show eight spots with angles in agreement

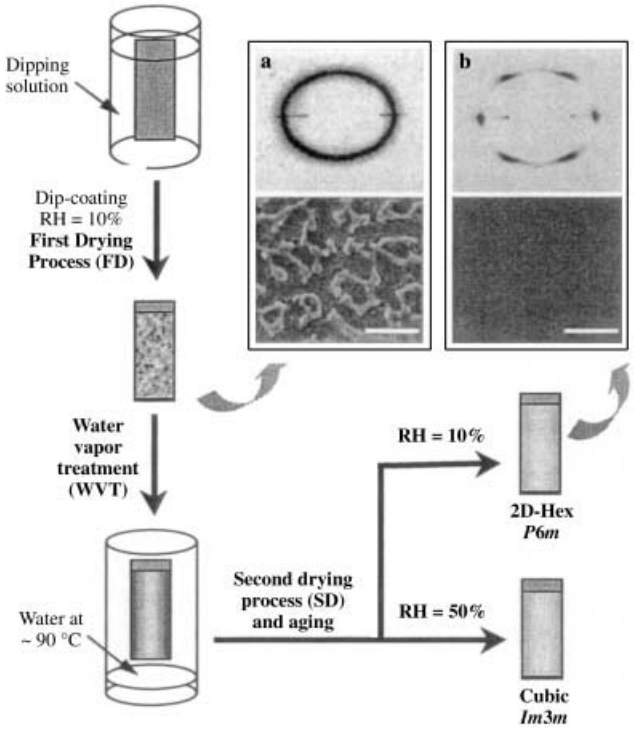

Figure 1. Schematic representation of film processing by dip-coating. Parts (a) and (b) are in situ SAXS patterns (top) and SEM images (bottom) acquired respectively before and after water vapor treatment. Scale bars are 10 μm.

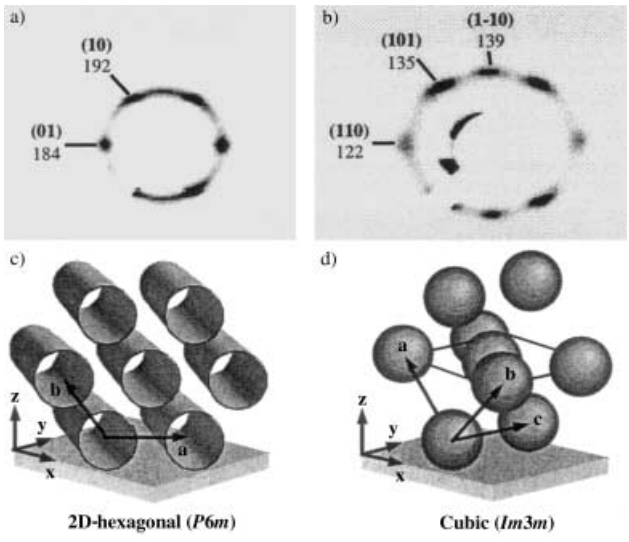

Figure 2. 2D SAXS patterns for F127-templated films: a) 2D hexagonal mesostructured CZ (drying and aging at RH = 10%); b) cubic mesostructured YZ (drying and aging at RH = 50%); c) and d) orientation scheme for the 2D hexagonal and cubic mesophases. Distances in parts (a) and (b) are given in Å.

 © 2003 Wiley-VCH Verlag GmbH & Co. KGaA, Weinheim 0044-8249/03/11503-0362 $ 20.00+.50/0

Table 1: Aging conditions and structural characteristics of Pluronic F127-templated films.

Inorganic framework	M/(M+Z)	RH [%]	Structure	*a* [Å]
ZrO_2	–	10	2D hexagonal	211
ZrO_2	–	50	2D hexagonal	218
ZrO_2–Y_2O_3	0.20	10	2D hexagonal	222
ZrO_2–Y_2O_3	0.20	50	cubic	197
ZrO_2–ceria	0.20	10	2D hexagonal	231
ZrO_2–ceria	0.20	50	cubic	213

with those between the {110} planes of a body-centered cubic mesophase (*Im*3*m* space group) with the (110) planes parallel to the substrate (see Figure 2c). A complete indexation for such a phase in the same orientation can be found elsewhere for F127-templated silica films.[14] This orientation seems to be the same as that reported for the Pluronic P123 (EO_{20}-$PO_{70}EO_{20}$, PO = propylene oxide) templated *Im*3*m* mesoporous silica and titania films.[15] Another orientation for this same structure, with the (100) planes parallel to the substrate, was also reported for F127-templated silica films.[16] For both 2D-hexagonal and cubic mesophases, SAXS patterns taken at incidence normal to the substrate displayed diffraction rings that show that the *c* vector (for both structures) does not have preferential orientation with respect to the deposition direction (*xy* plane, as represented in Figure 2c).

Transmission electron microscopy (TEM) images of calcined cubic and hexagonal films are presented in Figure 3.

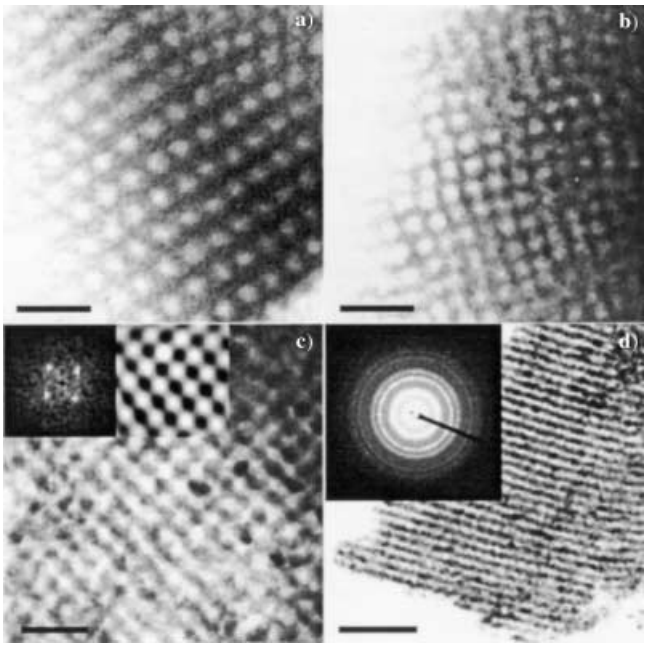

Figure 3. TEM images for F127-templated films: a) 2D hexagonal ZrO_2 treated at 300 °C; b) cubic CZ treated at 300 °C; c) and d) cubic YZ treated at 700 °C. The images are projections parallel to the following directions; [001] (a), [100] (b) and (c), and [211] (d). The insets in part (c) show the modulus of a Fourier-transform of the full image, and a reconstructed image of a selected region. The inset in part (d) is an electron diffraction pattern showing that the inorganic framework is composed of crystalline cubic YZ. Scale bars are: a) 25 nm, b) and c) 50 nm, and d) 100 nm.

Periodic distances are in agreement (within 10%) with those found by 2D SAXS (because of tilting or sample shrinking under calcination, see below). For cubic YZ and CZ, *a* values of 183 and 195 Å are found, respectively. In the case of hexagonal phases, an a_{TEM} value of around 200 Å was found for all compositions, which is in good agreement with the SAXS values, when considering the contraction upon thermal treatment.

The results described above show that for zirconia-based mixed-oxide systems, the final mesophase can be tailored by aging the film at controlled humidity. At high humidity, water is encouraged to remain inside the coating and is located within the inorganic network (through hydrogen bonding with OH groups and/or coordination to the metal cations), between the ABC hydrophilic chains, and at the organic–inorganic interface. These factors contribute to increase: 1) the inorganic/template volume ratio, 2) the curvature of the ABC micelles, and 3) the amount of interface.[14] During aging, further condensation progressively takes place (oxolation is thermodynamically favored),[11] which stabilizes the mesophase with varying quantities of water within the hybrid framework, to give three-dimensional (cubic, "humid" conditions) or two-dimensional (hexagonal, "dry" conditions) mesostructures. The results reported for silica–CTAB[17] and silica–F127 mesostructured films[14] are in agreement with the results reported here. It is recognized that the choice of the template[16] and the inorganic/template volume ratio are both important factors that determine the final mesostructure.[15] However, the results shown here and elsewhere[14,17] demonstrate clearly that the water content in the system is a crucial variable, and working without taking this parameter into account could lead to irreproducible results.

Films aged for 24 h are stable enough to be calcined without mesostructural transition. Heating induces further condensation, which stabilizes the coating and causes structural contraction. As a result of the adhesion of the film to the substrate, all the contraction should occur in the direction perpendicular to the substrate (*z* axis, as represented in Figure 2c). Such preferential (often uniaxial) contraction is well documented for mesostructured films exhibiting 2D hexagonal mesostructure (*P*6*m*),[13,18] but it has never been displayed for a cubic *Im*3*m* mesophase. The *P*6*m* distorted hexagonal structure can be described as a 2D-centered rectangular mesophase (*C*2*m*). The uniaxial contraction of the cubic *Im*3*m* mesostructure (Figure 1c) results in a considerable loss of symmetry. Formally, a triclinic unit cell can be found inside the distorted body-centered cubic mesostructure (see Supporting Information). For simplicity, the parameters of the cubic lattice (even after distortion), instead of those of the triclinic lattice, will be used here for the description of the structural changes.

SAXS data showed that the YZ and CZ cubic (or triclinic after contraction) mesostructures (Figure 4) are stable at temperatures as high as 700 °C. The (110) spots (the in-plane spots) become weak at 500 °C and above, which can be

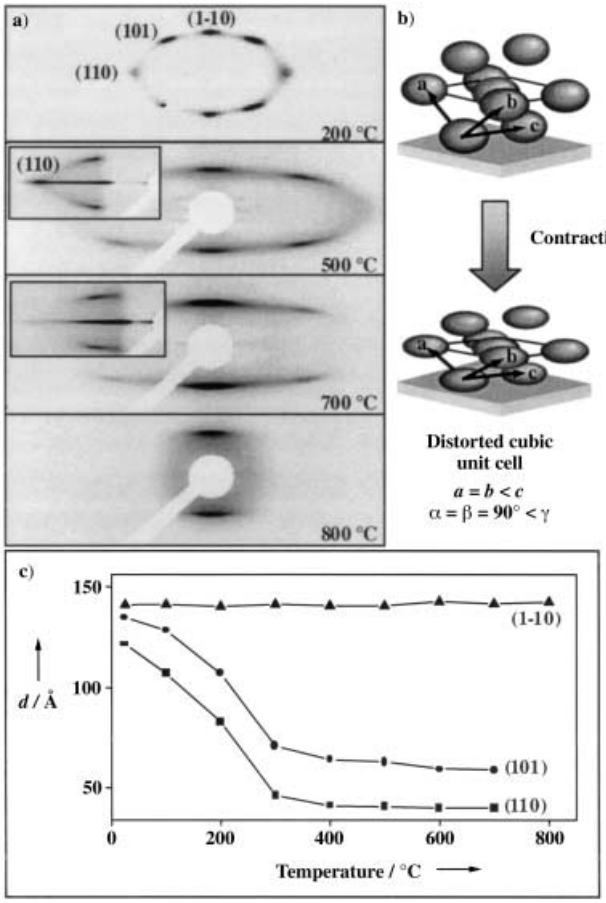

Figure 4. Typical results obtained during the calcination of films exhibiting a cubic mesostructure; the example here is a F127-templated YZ film. a) 2D SAXS patterns (4° incidence angle) of the film treated at different temperatures. The insets are patterns taken at a grazing incidence; b) schematic representation of the distorted cubic structure observed after the anisotropic contraction (the *c* parameter is constant); c) variation of *d* spacing as a function of temperature, which clearly displays the uniaxial contraction.

partially explained by the exponential decay of the reflection intensity on increasing Bragg angle for these large diffraction domains, and also by a reduction in structural order along the direction parallel to the substrate (remembering that such planes are subject to higher degrees of contraction). SAXS patterns collected in grazing incidence (see insets in Figure 4a) showed that the (110) spots are still present at 700 °C, although they are very weak. TEM images of films treated at 700 °C (Figure 3c and d) showed that the cubic (or triclinic) mesostructure is fully preserved. The inorganic framework remains continuous, and the cage-like pores (approximately 80 Å in diameter) can be observed throughout the sample (see Figure 3a). These values are close to those reported for SBA-16 (cavities of 95 Å),[19] and to those reported for F127-templated cubic (*Im*3*m*) silica films (85 Å).[16] In fact, after contraction the cage-like pores present themselves as ellipsoids of about 80 × 40 Å (parallel and perpendicular to the substrate, respectively). Such a high thermal stability for periodically organized transition-metal-oxide mesoporous materials has never been reported. Only disordered wormlike mesoporous metal oxides, such as YSZ,[5] Nb_2O_5,[20] and tungsten oxide–zirconia[21] are known to be stable after heating to temperatures in excess of 500 °C. Examples of nonsilicate periodically organized mesostructures stable up to 600 °C are only found for zirconium oxophosphates.[4,22] By 800 °C, only the (1–10) spots are still present in the SAXS patterns, which indicates that the initial order was retained only in the direction normal to the substrate. This loss of order can be seen by TEM (see Supporting Information), which shows a wormlike disordered structure, but with a constant correlation distance in one direction. Even though most of the order was lost, the porosity is still present at 800 °C.

2D hexagonal mesophases display lower thermal stability. At 400 °C a diffraction ellipse, together with the spots, can be observed in the SAXS patterns, independent of the inorganic composition, which indicates the presence of mixed organized and disorganized domains. The mesostructure degrades with increasing temperature, and completely polyoriented domains (only a diffraction ellipse is observed) are obtained after treatment at 700 °C for both YZ and CZ. For these 2D hexagonal mesophases, TEM investigations of films heated to 700 °C showed that the structure is really composed of disordered domains, and that the films are still porous.

For all inorganic compositions, electron diffraction (see inset in Figure 3d) and wide-angle X-ray diffraction (XRD) showed that crystallization commences at 300 °C. Very small crystallites (smaller than 2 Å) are initially detected (see Supporting Information). At 400 °C the inorganic walls are composed of cubic YZ (JCPDS 82–1245) or tetragonal CZ[23] crystallites with dimensions of 7–9 nm. These nanocrystallites do not significantly grow at temperatures up to 700 °C; the growth is likely to be hindered by the wall–pore boundaries. Heating to 800 °C causes the crystallites to grow to approximately 11 nm. The cubic or tetragonal zirconia-based mixed-oxide crystalline phase (respectively for YZ or CZ) is stable at temperatures above 1000 °C, and no phase segregation is observed. Stabilization of the cubic or tetragonal crystalline structure indicates that Y or Ce cations are well-dispersed inside the zirconia matrix.

A key to the high stability of the cubic mesophase seems to be the presence of large inorganic domains (which can be seen in the center of each four-pore square in Figure 3b and c). These domains, with dimensions of approximately 100–120 Å, can accommodate the large crystallites formed in the 400–700 °C temperature range.

For the 2D hexagonal mesophase, the lower thermal stability (of the structural order) can be attributed to the presence of inorganic walls with a thickness of around 80 Å. Notably, the main degradation of such a mesostructure occurs together with the crystallite growth (400–500 °C, where polyoriented domains begin to appear). Therefore, the mesostructural degradation can be directly related to the formation of crystallites that exceed the size of the inorganic framework domains.

Thermogravimetric and differential scanning calorimetry analysis (TGA–DSC) showed that in air, most of the template is lost from 200 to 400 °C for all inorganic compositions. FT-IR investigations confirmed that films treated at 400 °C are free of organic compounds (see Supporting Information). The

 © 2003 Wiley-VCH Verlag GmbH & Co. KGaA, Weinheim 0044-8249/03/11503-0364 $ 20.00+.50/0

thickness of these films was estimated by SEM and TEM to be around 300 nm (for a withdrawal rate of 1.5 mm s^{-1}). Successive coatings can be applied (four coatings have been achieved) after stabilization at 130–150 °C, which gives rise to crack-free films that exhibit good optical quality. Preliminary results showed that other templates, such as Brij 56 or 58 surfactants (C_nEO_m), are suitable for the preparation of mesoporous YZ and CZ thin films, which allow the formation of smaller pores (20–40 Å) than those obtained with F127.

In summary, the formation of highly organized mesoporous yttria–zirconia and ceria–zirconia thin films is demonstrated for the first time. The mesostructure can be controlled by the conditions applied in the post-processing of the film; cubic or 2D hexagonal mesophases are formed by varying the quantity of water inside the coating during aging. 2D hexagonal mesostructures are stable to 400–500 °C. In addition to the loss of periodicity, the porosity is conserved up to at least 800 °C (the highest temperature investigated) for both mesophases. The cubic mesostructures are stable to 700 °C, which represents the highest thermal stability reported so far for periodically organized mesoporous transition-metal-oxide materials. The resulting porous inorganic framework is highly crystalline, and is composed of cubic YZ or tetragonal CZ. These robust, 3D-interconnected porous coatings, which are prepared by a very convenient one-pot sol-gel method, are very promising. Moreover, the chemical concepts developed in this work can be easily extended to the preparation of YZ and CZ mesoporous particles at the micron or submicron scale[24] as we have demonstrated that the methods developed to prepare mesoporous transition-metal-oxide thin films could feasibly be employed for the formation of spherical particles using aerosol techniques.[25] Therefore, this study presents new opportunities for designing shape-tailored mesoporous materials for applications such as heavy-duty conductive membranes, catalysis, sensors, and electrode materials.

Experimental Section

The dipping solutions were prepared by reacting a mixture of metal chlorides (MCl_3 + $ZrCl_4$, M = Y or Ce; 0.01 mol) with an ABC solution (Pluronic F127 ($EO_{106}PO_{70}EO_{106}$), 0.005 mol) in EtOH (0.4 mol). Water was added to this mixture (20:1 H_2O/metal molar ratio), which resulted in very acidic (less than pH 0) solutions that prevented precipitation. Films were prepared by dip-coating glass or silicon substrates at a constant withdrawal rate (1–5 mm s^{-1}) under controlled relative humidity (RH = 10 %) and temperature (20–23 °C). Immediately after the first drying process (see Figure 1), films were submitted to a water-vapor treatment for 10–20 s. Subsequently, the second drying process took place inside the chamber of the dip-coater under controlled RH (either 10 or 50 %) in flowing air for 1 h. Thereafter, films were transferred to an RH-controlled (using saturated solutions of different salts) closed chamber and aged for between 12 h and 2 weeks. SD and aging were carried out at a controlled temperature (20–22 °C). After aging, films were calcined in static air at temperatures in the 100–800 °C range (ramping rate of 1 °C min^{-1}) for 4 h.

Received: September 12, 2002 [Z50147]

[1] T. Takahashi, N. Q. Minh, *Science and Technology of Ceramic Fuel Cells*, Elsevier, New York, **1995**.

[2] M. Daturi, C. Binet, J.-C. Lavalley, A. Galtayries, R. Sporken, *Phys. Chem. Chem. Phys.* **1999**, *1*, 5717, and references therein.

[3] B. C. H. Steele, *Nature* **1999**, *400*, 619.

[4] a) C. T. Kresge, M. E. Leonowicz, W. J. Roth, J. C. Vartuli, J. S. Beck, *Nature* **1992**, *359*, 710; b) C. G. Göltner, M. Antonietti, *Adv. Mater.* **1997**, *9*, 431; c) J. Y. Ying, C. P. Mehnert, M. S. Wong, *Angew. Chem.* **1999**, *111*, 58; *Angew. Chem. Int. Ed.* **1999**, *38*, 56; d) F. Schüth, *Chem. Mater.* **2001**, *13*, 3184; e) G. J. de A. A. Soler-Illia, C. Sanchez, B. Lebeau, J. Patarin, *Chem. Rev.* **2002**, in press.

[5] a) M. Mamak, N. Coombs, G. Ozin, *Adv. Mater.* **2000**, *12*, 198; b) M. Mamak, N. Coombs, G. Ozin, *J. Am. Chem. Soc.* **2000**, *122*, 8932.

[6] a) Y. Wang, L. Yin, O. Palchik, Y. Rosenfeld Hacohen, Y. Koltypin, A. Gedanken, *Chem. Mater.* **2001**, *13*, 1248; b) Y. Q. Wang, L. X. Yin, O. Palchik, Y. Rosenfeld Hacohen, Y. Koltypin, A. Gedanken, *Langmuir* **2001**, *17*, 4130.

[7] a) C. J. Brinker, Y. Lu, A. Sellinger, H. Fan, *Adv. Mater.* **1999**, *11*, 579; b) P. Yang, D. Zhao, D. I. Margolese, B. F. Chmelka, G. D. Stucky, *Nature* **1998**, *395*, 583; c) G. J. de A. A. Soler-Illia, A. Louis, C. Sanchez, *Chem. Mater.* **2002**, *14*, 750.

[8] a) D. Grosso, F. Babonneau, P.-A. Albouy, H. Amenitsch, A. R. Balkenende, A. Brunet-Bruneau, J. Rivory, *Chem. Mater.* **2002**, *14*, 931; b) E. L. Crepaldi, D. Grosso, G. J. de A. A. Soler-Illia, P.-A. Albouy, H. Amenitsch, C. Sanchez, *Chem. Mater.* **2002**, *14*, 3316.

[9] D. Grosso, A. R. Balkenende, P.-A. Albouy, A. Ayral, H. Amenitsch, F. Babonneau, *Chem. Mater.* **2001**, *13*, 1848.

[10] E. L. Crepaldi, G. J. de A. A. Soler-Illia, D. Grosso, P.-A. Albouy, H. Amenitsch, C. Sanchez, *Stud. Surf. Sci. Catal.* **2002**, *141*, 235.

[11] E. M. Larsen, in *Advances in Inorganic Chemistry and Radiochemistry, Vol. 13* (Eds.: H. J. Emeléus, A. G. Sharpe), Academic Press, New York, **1970**, p. 1.

[12] E. L. Crepaldi, G. J. de A. A. Soler-Illia, D. Grosso, P.-A. Albouy, C. Sanchez, *Chem. Commun.* **2001**, 1582.

[13] M. Klotz, P.-A. Albouy, A. Ayral, C. Ménager, D. Grosso, A. Van der Lee, V. Cabuil, F. Babonneau, C. Guizard, *Chem. Mater.* **2000**, *12*, 1721.

[14] G. J. de A. A. Soler-Illia, E. L. Crepaldi, D. Grosso, D. Durand, C. Sanchez, *Chem. Commun.* **2002**, 2298.

[15] P. C. A. Alberius, K. L. Frindell, R. C. Hayward, E. J. Kramer, G. D. Stucky, B. F. Chmelka, *Chem. Mater.* **2002**, *14*, 3284.

[16] D. Zhao, P. Yang, N. Melosh, J. Feng, B. F. Chmelka, G. D. Stucky, *Adv. Mater.* **1998**, *10*, 1380.

[17] F. Cagnol, D. Grosso, G. J. de A. A. Soler-Illia, E. L. Crepaldi, C. Sanchez, *J. Mater. Chem.*, **2003**, in press.

[18] D. Grosso, G. J. de A. A. Soler-Illia, F. Babonneau, C. Sanchez, P.-A. Albouy, A. Brunet-Bruneau, A. R. Balkenende, *Adv. Mater.* **2001**, *13*, 1085.

[19] Y. Sakamoto, M. Kaneda, O. Terasaki, D. Y. Zhao, J. M. Kim, G. Stucky, H. J. Chin, E. Ryoo, *Nature* **2000**, *408*, 449.

[20] B. Lee, T. Yamashita, D. Lu, J. N. Kondo, K. Domen, *Chem. Mater.* **2002**, *14*, 867.

[21] M. S. Wong, E. S. Jeng, J. Y. Ying, *Nano Lett.* **2001**, *1*, 637.

[22] U. Ciesla, M. Fröba, G. Stucky, F. Schüth, *Chem. Mater.* **1999**, *11*, 227.

[23] S. Rossignol, Y. Madier, D. Duprez, *Catal. Today* **1999**, *50*, 261.

[24] Preliminary results showed that by using the same conditions that were applied to prepare mesoporous thin films, mesoporous CZ submicronic particles can be obtained by aerosol processing (see Supporting Information).

[25] D. Grosso, G. J. de A. A. Soler-Illia, E. L. Crepaldi, C. Sanchez, *Adv. Funct. Mater.* **2003**, in press.